SELECTIVE NICKEL-IRON SEPARATION FROM ATMOSPHERIC LEACH LIQUOR OF A LATERITIC NICKEL ORE USING THE PARA-GOETHITE METHOD

Huseyin BASTURKCU, Neset ACARKAN

Istanbul Technical University, Mining Faculty, Mineral Processing Engineering Department, Istanbul, Turkey
basturkcu@itu.edu.tr

Abstract: The presence of iron in pregnant leach solutions (PLS) is a common problem, and is generally removed using jarosite, goethite, hematite or para-goethite precipitation methods. Although these methods are successfully applied, significant amounts of nickel can be lost. In this study, iron precipitation was performed on a PLS obtained from agitation leaching of a lateritic nickel ore under atmospheric conditions using the para-goethite method. The PLS contained 2.62 g/dm^3 Ni, 54.28 g/dm^3 Fe and 0.14 g/dm^3 Co. During the precipitation tests the effect of pH, time, temperature, and metal concentration were investigated. The influence of the key points, temperature and metal concentration, on nickel loss was explained in reference to SEM and XRD analyses. Ultimately, selective nickel and iron separation was achieved with complete iron precipitation and only 1.2% Ni loss.

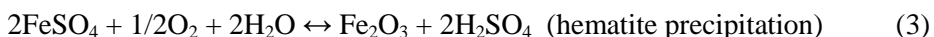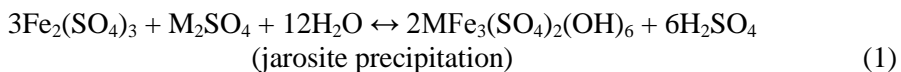*Keywords: iron precipitation, nickel loss, para-goethite method*

Introduction

Nickel is generally found as an associated form with iron oxides in nickeliferrous limonites $(Fe,Ni)O(OH)·nH_2O$. Nickel existing in this structure can only be released by acid attack. Therefore, nickel extraction is strongly related with the decomposition of iron matrix, which causes high acid consumptions (Chang et al., 2010). Meanwhile, atmospheric acid leaching of lateritic nickel ores has increased in importance, as the general capital costs are higher in pressure acid leaching operations (McDonald and Whittington, 2008).

The associated structure of nickel and iron in minerals such as goethite and limonite results in high iron content in the pregnant leach solution (Buekes et al., 2000). Iron presence in many beneficiated materials is a common case since iron is one of the most abundant elements on earth. Likewise in zinc industry, zinc concentrates generally contain 3-18% iron (Chen and Cabri, 1986). Iron removal

methods from pregnant leach solutions of laterites are adopted from the zinc industry. Iron is usually removed from leaching solutions by precipitation.

Precipitation methods of goethite (Allen et al., 1970; Bodson, 1972; Boxal and James, 1986; Torfs and Vliegen, 1996), hematite (Ropenack, 1986; Onazaki and Kuramochi, 1986; Mealey, 1973) and jarosite (Pickering and Haigh, 1970; Steintveit, 1971; Haigh and Wood, 1972; Arregi et al., 1980; Scott et al., 1986; Tamargo et al., 1996; Buban et al., 1999) have found place in industrial applications up today. In addition, carbonate, hydroxide, sulfide, and oxidative precipitation methods are being investigated in the literature (Pakarinen and Paatero, 2011).

It was reported that the jarosite process has economical disadvantageous due to the high cost of impounding. In other respects, no further needs for alkali addition, low volume and relatively stable residue can be counted as the advantages for goethite precipitation (Ismael and Carvalho, 2003; Chang et al., 2010). The Union Miniere (Torfs and Vliegen, 1996) indicated that goethite process offers some possibilities for further treatment to obtain an inert material, which resulted in a possible usage in construction industry. In terms of hematite precipitation, although the precipitated hematite can be used as a marketable iron product, the precipitation process needs temperature above 100 $^{\circ}$C, which refers to high capital and operational costs. The occurring reactions of these methods are given in Eqs. 1, 2, and 3 (Ismael and Carvalho, 2003).

$$3Fe_2(SO_4)_3 + M_2SO_4 + 12H_2O \leftrightarrow 2MFe_3(SO_4)_2(OH)_6 + 6H_2SO_4$$
$$\text{(jarosite precipitation)} \tag{1}$$

$$Fe_2(SO_4)_3 + 4H_2O \leftrightarrow 2FeOOH + 3H_2SO_4 \quad \text{(goethite precipitation)} \tag{2}$$

$$2FeSO_4 + 1/2O_2 + 2H_2O \leftrightarrow Fe_2O_3 + 2H_2SO_4 \quad \text{(hematite precipitation)} \tag{3}$$

Besides the jarosite, goethite, and hematite methods, the so-called para-goethite method has also become a topic for the studies. The para-goethite process was started operating by Zinifex at the Hobart smelter. The residue, which was not a documented mineral, was treated in lead sintering (McCristal et al., 1998). Meyer et al. (1996) indicated that 40% of iron precipitate was amorphous, and by this, the character of its phases could not be determined. However, the phases were thought to be goethite with poor crystalline structure. Until Loan et al. (2002) study, not so much was known about the nature of the para-goethite residue (Cubeddu et al., 1996; McCristal et al., 1998). Loan et al. (2002, 2006) identified 6-line ferrihydrite to be the major precipitated iron phase. The conditions for the precipitation of hematite, goethite, ferric hydroxide, and hydroxyl salts are shown in Table 1.

With regard to the para-goethite method, it requires nearly pH 3 and 80 $^{\circ}$C temperature to provide the iron precipitation. While it can be defined as a type of the goethite method, the character of its iron precipitate makes it different.

Table 1. Conditions for precipitation of hematite, goethite,
ferric hydroxide and hydroxyl salts (based on Babcan, 1971)

Species	pH	Temperature (^{o}C)
Fe^{3+}	0-1	0-70
	1-2	25-80
Fe(OH)$_3$	3-6	35-40
	6-10	10-35
Hydroxy Salts	0-1	>80
	1-3	<80
Hematite	2-8	>100
Goethite	3-8	40-80
Paragoethite	3-4	70-90

Solvent extraction has been widely studied in treatment of iron from metal solutions (Sato and Nakamura, 1971; Hoh et al., 1983; Demopoulos and Gefvert, 1984; Vazarlis and Neou-Syngoyna, 1984; Preston, 1985; Sato et al., 1985; Biswas and Begum, 1998; Saji et al., 1998; Zhou et al., 1989; Ritcey, 2006). In solvent extraction, the basic encountered problem is stripping which needs strong acid and reduction (Demopoulos and Gefvert, 1984; Vazarlis and Neou-Syngoyna, 1984; Lupi and Pilone, 2000). The strong acid usage poses a risk for reagent decomposition. In the presence of high iron content, solvent extraction becomes less economical (Pakarinen and Paatero, 2011).

Nickel loss

The nickel loss during the iron precipitation might be attributed to two mechanisms: adsorption or co-precipitation (Singh et al., 2002; Carvalho-E-Silva et al., 2003) due to physical or chemical bonding (Beukes et al., 2000). It is thought that the main reason is adsorption (Agatzini-Leonardou et al., 2009).

The products of different precipitation processes have adsorption ability. While the adsorption capability of synthetic goethite and hematite samples was shown in a study of Buekes et al. (2000), ferrihydrite is also known as an adsorbent for many inorganic and organic species (Jambor and Dutrizac, 1998). Besides, depending on the changes in pH, temperature, and water activity, ferrihydrite can transform to more crystalline products of goethite (α-FeOOH) and hematite (α-Fe$_2$O$_3$) (Loan et al., 2006).

The adsorption mechanism has been explained considering physical parameters, particle size, and BET surface area of the precipitates. It is known that surface area affects the adsorption process, and there is an inverse relationship between surface area and particle size (Cornell and Schwertmann, 1996). Furthermore, the higher initial Fe/Ni ratio causes more nickel loss which results in the increase of the precipitate amount. When the same initial Fe/Ni ratio was tested at different pH values, remarkable nickel loss was observed by increasing pH (Chang et al., 2010).

In this context, the aim of this study was to provide an enhancement in selective nickel-iron separation from atmospheric leach liquor of a lateritic nickel ore using the para-goethite precipitation method.

Experimental

PLS used for the precipitation tests in this study was obtained as a product of agitation leaching of a lateritic nickel ore with sulfuric acid under atmospheric conditions (Basturkcu and Acarkan, 2016). The metal contents of the PLS were found to be 2.62 g/dm^3 Ni, 54.28 g/dm^3 Fe, and 0.14 g/dm^3 Co.

The precipitation tests were conducted in a heated reaction vessel. Slaked lime (pulp calcium hydroxide – $Ca(OH)_2$) was used to adjust the pH value of the solution which was measured by a pH-meter with a temperature resistant glass electrode. Solid-liquid separation was performed using a Buchner funnel, and the metal content of the remaining solution was analyzed by Atomic Absorption Spectrophotometer (AAS). Additionally, X-Ray Diffraction (XRD) and scanning electron microscope (SEM) analyses were performed on the dried precipitates in order to determine the changes in their chemical and mineralogical structure.

In the precipitation tests, the effect of pH, time, temperature, and metal concentration were investigated. The chemical changes in the precipitates were examined in detail. According to the results, a solution for preventing the nickel loss was suggested.

Results and discussion

Results

Effect of pH

The effect of pH on the iron precipitation was investigated at different pH values of 2.5, 3.0, 3.5, 4.0, and 5.0. Each of the precipitation experiments took 60 min without the heating. However, the temperature increased with the addition of $Ca(OH)_2$ because a chemical reaction occurring between the acidic medium and alkaline additive. At that moment, it should be reported that the speed of the added lime was critical to control the precipitation process.

As seen from Fig. 1, 99% iron precipitation was achieved with significant amounts of nickel and cobalt losses at pH 3.0. As long as the pH increased, the losses in nickel and cobalt continued increasing. According to the results, the optimum pH value was determined at 3, and the precipitation time was decided to be examined.
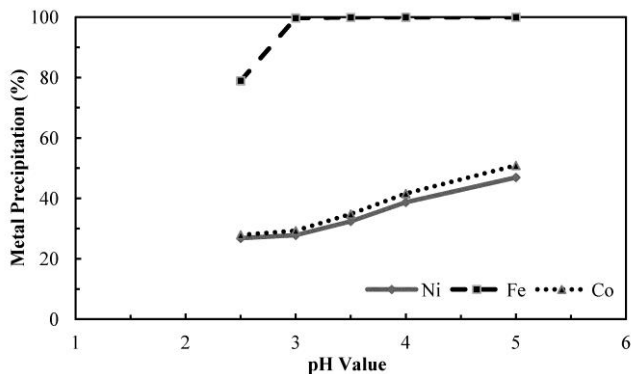
Fig. 1. Effect of pH on iron precipitation (60 min, without heating)

Effect of precipitation time

To investigate the effect of time on the metal precipitations, the tests were carried out at pH 3 without the heating. The times of 30, 60, 90, and 120 min. for the precipitations were applied on the PLS. As shown in Fig. 2, there are slight differences in the metal concentrations, however at 60 min of precipitation, 99.9% Fe precipitation was achieved with 27.8% Ni and 29.3% Co losses. In comparison with 30 min, it could be indicated that the nickel and cobalt losses decreased 3.5% and 3.1%, respectively. When 90 and 120 min were applied, the losses were as nearly the same as 60 min did. Therefore, 60 min was chosen as the optimum time for the further tests.
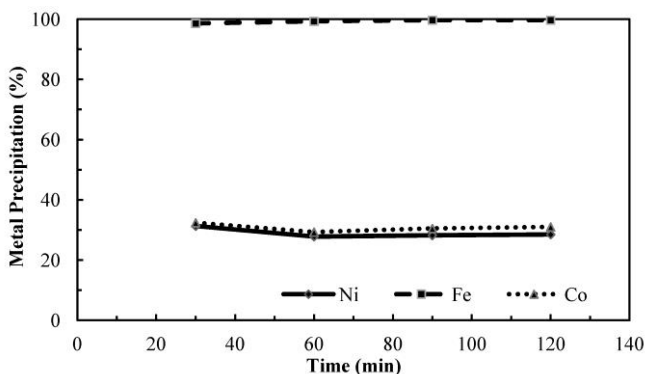

Fig. 2. Effect of precipitation time (pH 3, without heating)

Effect of temperature on metal concentration

Up to this part of the study, the complete iron precipitation was obtained with high amounts of nickel and cobalt losses. For this reason, in this part, efforts were made to decrease these losses. Temperatures of 50, 60, 70, 80, and 90 ^{o}C were tested for each metal concentration: 1.31 g/dm^3 Ni, 27.14 g/dm^3 Fe and 0.07 g/dm^3 Co (A); 2.62

g/dm^3 Ni, 54.28 g/dm^3 Fe and 0.14 g/dm^3 Co (*B*); 5.24 g/dm^3 Ni, 108.56 g/dm^3 Fe and 0.28 g/dm^3 Co (*C*).

The tests were carried out for 60 min, and the obtained results are shown in Figs. 3, 4, and 5 with regard to nickel, cobalt, and iron. In terms of iron, the iron precipitation process could not be completed for the metal concentrations of *B* and (C) until 80 ^{o}C. However, the increase in the temperature showed a positive effect on iron precipitation under these concentrations. On the other hand, 99.9% Fe precipitation was achieved with the metal concentrations of *A* at all temperatures. Therefore, an evaluation on the nickel and cobalt losses was necessary in order to compare the effect of temperature on the metal concentration.

While the losses had a downward trend as the temperature increased, the sharp difference between the nickel losses could be observed. When the concentration *C* was used, 27.1% Ni loss decreased to 14.3% Ni as the temperature was increased from 50 ^{o}C to 90 ^{o}C. On the other hand, 80 ^{o}C temperature was found to be sufficient for the complete iron precipitation with only 1.2% Ni loss when the metal concentration *B* was diluted to that of *A*. In this way, there was no need to increase the temperature to 90 ^{o}C. From cobalt point of view, the loss of 26.7% with the concentration *C* decreased to 14.2% at 90 ^{o}C. Also, concentration *A* provided just 1.5% Co loss at 80 ^{o}C.

The final iron precipitate was chemically analysed to determine the residual elements. As presented in Table 2, the nickel and cobalt contents in the iron precipitate were almost zero. Meanwhile, there were not large quantities of Mg or Al in the precipitate. On the contrary, calcium showed a highest content of 17.28% due to the lime addition.

Table 2. Chemical analyses of final iron precipitate (80 ^{o}C, 60 min, pH 3)

Fe (%)	Ni (%)	Co (%)	Mg (%)	Ca (%)	Al (%)	*LOI (%)
8.90	0.015	<0.001	0.034	17.28	0.862	9.66

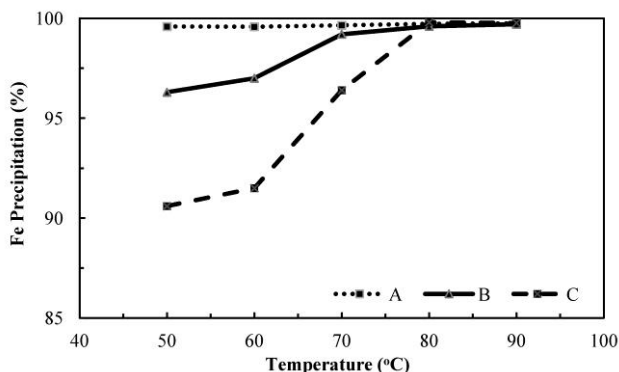* Loss of ignition at 1000 ^{o}C

Fig. 3. Effect of temperature on iron precipitation (60 min, pH 3)
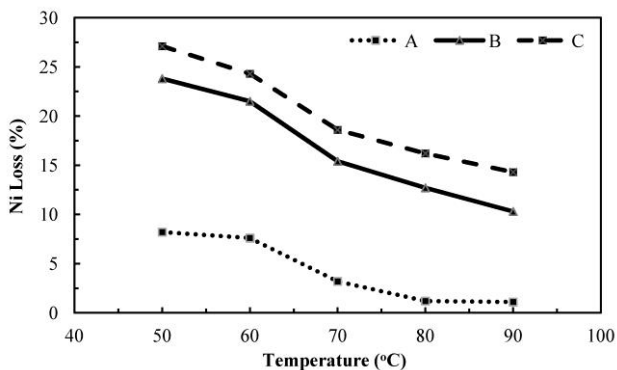
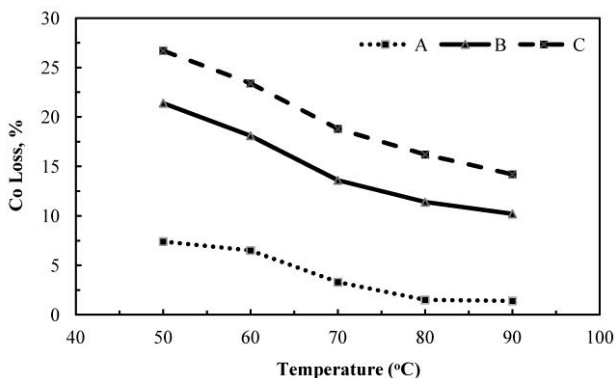Fig. 4. Effect of temperature on nickel loss (60 min, pH 3)

Fig. 5. Effect of temperature on cobalt loss (60 min, pH 3)

Based on the results obtained, it was possible to establish a flow-sheet including temperature and dilution in the precipitation process. Figure 6 shows the whole leaching process for the laterite ore sample. The iron precipitation part was performed at 80 $^{\circ}$C using lime on the diluted PLS. When a selective separation of iron and nickel-cobalt was achieved, then nickel and cobalt were separated from the solution. The barren solution was subsequently recycled to the iron precipitation step as to dilute the PLS.

Characterization of precipitates

After all, it was necessary to explain the precipitation mechanism by the means of XRD and SEM analyses performed on three iron precipitates: Before heating (concentration *B*), after treatment at 90 $^{\circ}$C (concentration *B*), and after treatment at 80 $^{\circ}$C (concentration *A*). Figures 7, 8, and 9 show the XRD analyses of these samples. The SEM images can be seen in Fig. 11.
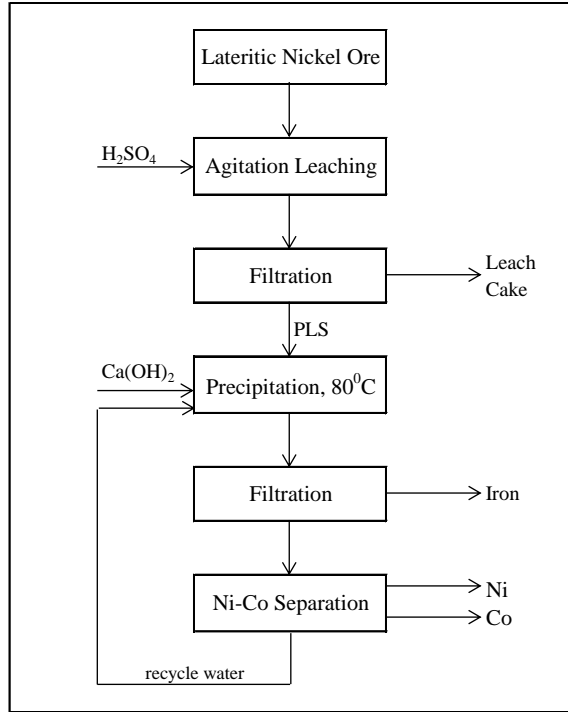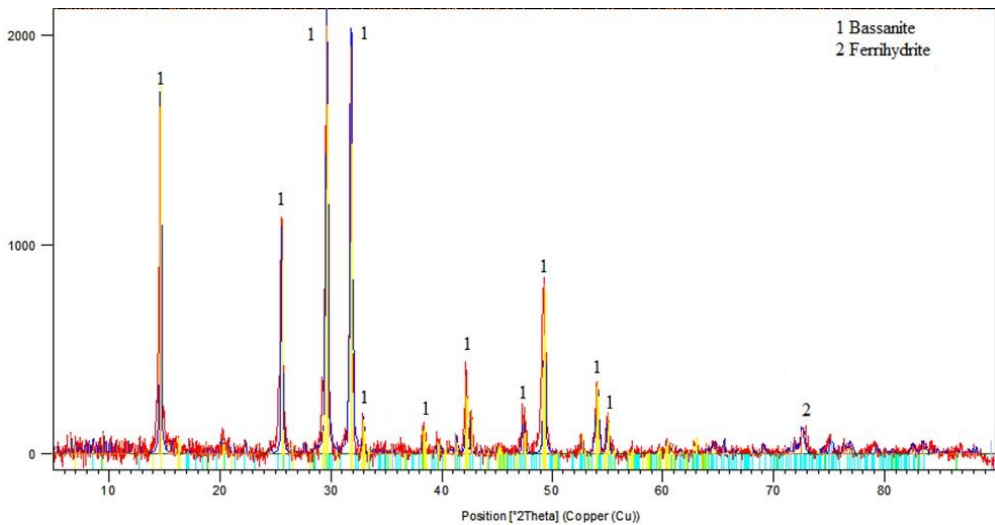
Fig. 6. Flow-sheet of precipitation process

Fig. 7. XRD analyses of the precipitate before temperature treatment (metal concentration *B*)

According to the XRD analyses of the samples, when temperature was not increased during the precipitation process, basically bassanite–$CaSO_4 \cdot 0.5(H_2O)$ was

formed with lesser amounts of ferrihydrite – $Fe_2O_3 \cdot 0.5(H_2O)$. When hearting was applied, ferrihydrite and bassanite peaks weakened and gypsum formation was observed.
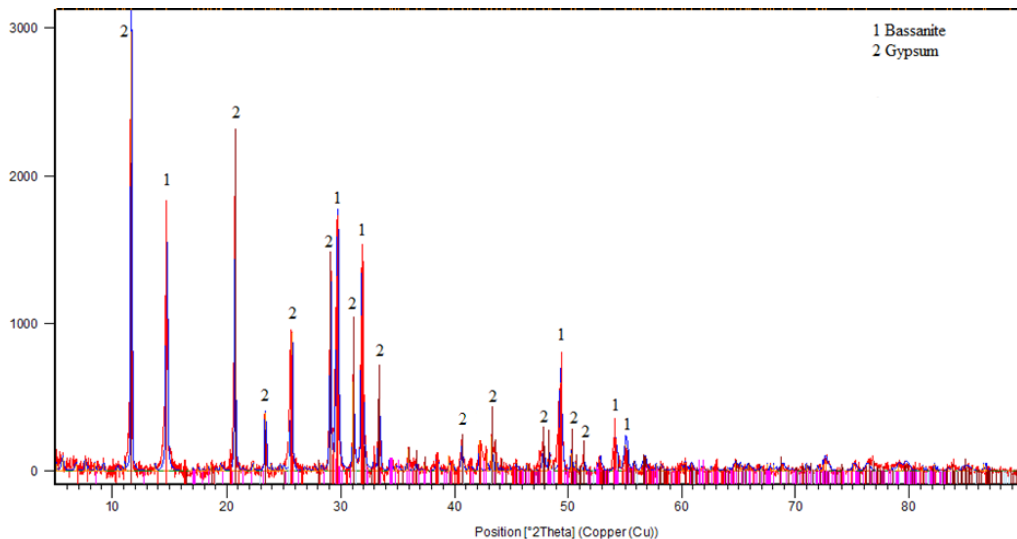

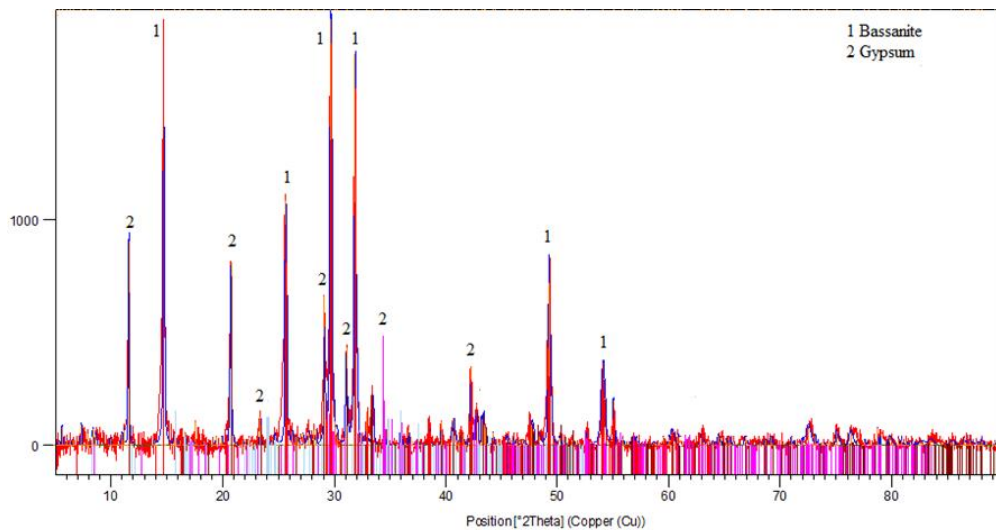Fig. 8. XRD analyses of the precipitate after 90 °C treatment (metal concentration *B*)

Fig. 9. XRD analyses of the precipitate after 80 °C treatment (metal concentration *A*)

Ferrihydrite is a hydrated ferric iron compound and occurs naturally or can be synthesized by rapid hydrolysis of Fe^{3+} solution (Schwertmann and Cornell, 1991). Basically, ferrihydrite is formed in two ways indicated by: i) two scattering bands in

its most disordered state, ii) a maximum of six strong lines in its most crystalline state. The difference between these 2-line and 6-line ferrihydrites is the size of the constitutive crystallites (Manceau and Drits, 1993).

In a study of Wang et al. (2011), nickel loss from synthetic atmospheric leaching liquors was investigated, and the precipitates were found to be dominated by ferrihydrite and/or schwertmannite. These oxyhydroxide and oxyhydroxysulphate iron compounds were thermodynamically unstable, and had poor crystallinity, and tend to transform to more stable iron oxides as a function of time. Since the crystal structures and basic properties of these minerals have not been determined yet, mineralogical identifications become difficult (Cornell and Schwertmann, 2003).

The XRD patterns of schwertmannite and 6-line ferrihydrite show similarities. They can have strong peaks at around 41° 2θ and two weaker peaks between 70° and 80° 2θ. While schwertmannite causes two other peaks at around 21° and 31° 2θ, 6-line ferrihydrite exhibits distinctive peaks at around 47° 2θ (Wang et al., 2013).

The ferrihydrite peaks shown in Fig. 7 (between 70° and 80° 2θ) are less distinctive when compared to these shown in Fig. 8 because more amorphous precipitates were formed. Dyer et al. (2012) found a similar result, and explained that higher temperature and low pH lead to more rapid hydrolysis resulting in the formation of finer particles, which seem to be more amorphous. In addition, they emphasized that less crystalline species were formed by increasing temperature from 35 to 45 $^{\circ}$C, which is favorable in industrial operations. Furthermore, as the temperature increased, more amorphous phases were observed in our study.
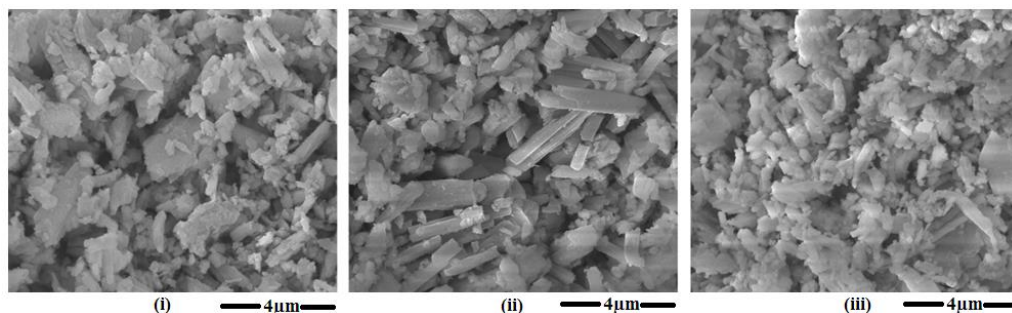

Fig. 10. SEM images of i) before temperature treatment (concentration *B*), ii) after 90 $^{\circ}$C treatment (concentration *B*), and iii) after 80 $^{\circ}$C treatment (concentration *A*)

In terms of calcium sulphate compounds, increasing solution temperature leads to gypsum formation with lesser amount of bassanite. The XRD analyses were approved by the images given in Fig. 10. As the temperature increased, the amount of bassanite was smaller, and a needle shaped gypsum particles was observed.

Additionally, the precipitates, which were obtained in the absence of temperature treatment, were partly coarse with sizes varying from 0.5 mm to 1 mm. By using hot and dilute solution in the precipitation tests, the degree of supersaturation decreased,

and the coarse particles formation with the crystal formation were prevented. The precipitate showed an amorphous structure. It made it difficult to determine ferrihydrite in the XRD analysis. It should be emphasized that the formation of calcium compounds and particle size of the crystals depended on the solution temperature and metal concentration. According to Fig. 10, the following findings were determined.

1. In the absence of temperature treatment, flat shaped bassanite minerals were observed having about 3 µm crystal size. Meanwhile, the size of the gypsum crystals was about 2-3 µm size.
2. The size and amount of the bassanite crystals decreased and mainly a needle shaped gypsum was observed.
3. By heating and dilution the crystal size of the gypsum decreased.

Discussion

As mentioned before, the nickel loss during iron precipitation might be attributed to adsorption or co-precipitation, while the main reason is believed to be adsorption. Nevertheless, it is difficult to determine whether it is adsorption or co-precipitation.

From the point of view of adsorption, Dyer et al. (2012) reported that ferrihydrite has a greater surface area and porosity than the most of the iron oxide minerals. The specific surface area of ferrihydrite is several hundred square meters per gram and ferrihydrite has also high density of local or point defects. These properties bring high ability to adsorb many chemical species (Waychunas et al., 1993; Fuller et al., 1993; Welch et al., 2000; Hochella et al., 2005). According to our findings, as more amorphous precipitates were formed, less nickel loss was observed. It is known that the adsorption ability of amorphous materials is higher. Thus, two phenomena can be suggested: i) calcium sulfate compounds, mostly gypsum, masked the surfaces of ferrihydrite and prevented adsorption, ii) the reason of nickel loss is not adsorption.

There are three fundamentals of co-precipitation: inclusion, occlusion, and adsorption. Inclusion is a co-precipitated impurity, which occupies a lattice site in the precipitate. Potential interfering ions, whose radius and charge are similar to carrier ion, may substitute into the lattice structure by chemical adsorption. Occlusion occurs when physically adsorbed interfering ions are trapped within a precipitate during its formation. Sometimes a part of solution is trapped in the growing precipitate with the effect of rapid precipitation. Adsorbate is an impurity weakly bounded to the surface of the precipitate chemically or physically (Harvey, 2000). Illustrative diagram of co-precipitation is given in Fig. 11.

The authors of this paper overemphasize the amorphous structure of the precipitates, since the amorphous constituents can mask the surface of the adsorbent mineral. This might hinder adsorption or provide a less crystalline precipitate, which prevents occlusion.
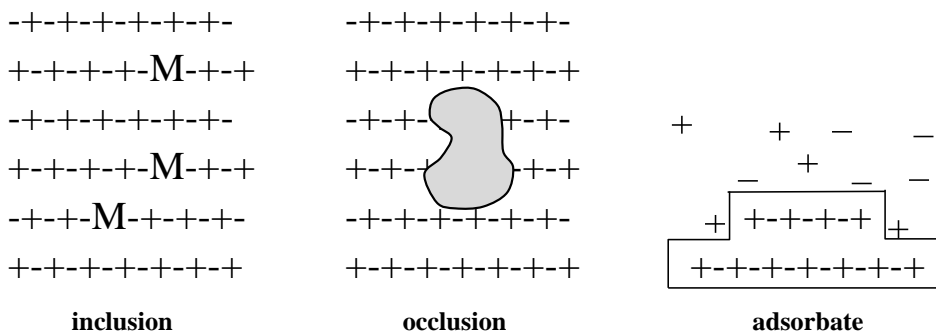
```
-+-+-+-+-+-+-          -+-+-+-+-+-+-
+-+-+-+-M-+-+          +-+-+-+-+-+-+
-+-+-+-+-+-+-          -+-+-        -+-+-
+-+-+-+-M-+-+          +-+-+-       +-+
-+-+-M-+-+-+-          -+-+-+-+-+-+-
+-+-+-+-+-+-+          +-+-+-+-+-+-+
   inclusion              occlusion                 adsorbate
```

Fig. 11. Example of co-precipitation: (+) and (-) represent the cation–anion,
M is the impurity (adopted from Harvey, 2000)

Conclusion

The para-goethite precipitation method was applied for atmospheric leach liquor of a lateritic nickel ore. The PLS contained 2.62 g/dm^3 Ni, 54.28 g/dm^3 Fe and 0.14 g/dm^3 Co. In the tests, the effect of pH, temperature, and metal concentration were investigated. As result, total iron precipitation with 1.2% Ni and 1.5% Co losses was achieved. To obtain this result, the PLS was diluted 1:1 by volume and precipitated at pH 3 and 80 $^\circ$C for 60 min. According the XRD and SEM analyses, mainly ferrihydrite and calcium sulfate minerals were formed in the precipitate. As the temperature increased, lesser bassanite and greater gypsum formation were observed in the amorphous precipitate. Together with amorphous precipitate formation, it became difficult to determine ferrihydrite.

In conjunction with the mineralogical observations and chemical results, possible reasons for nickel loss were explained. Due to heating and lower metal concentration, the size of crystals of the precipitate decreased and adsorption and/or occlusion of nickel was prevented. Also, it was concluded that the size and shape of the precipitated crystals had effect on nickel loss.

References

AGATZINI-LEONARDOU S., TSAKIRIDIS P.E., OUSTADAKIS P., KARIDAKIS T. and KATSIAPI A. 2009, *Hydrometallurgical process for the separation and recovery of nickel from sulphate heap leach liquor of nickeliferrous laterite ores*, Minerals Engineering 22, 1181–1192.

ALLEN R.W., HAIGH C.J. and HAMDORF C.J., 1970, *An improved method of removing dissolved ferric iron from iron-bearing solution*, Australian Patent No. 424, 095.

ARREGI V., GORDON A.R. and STEINVEIT G., 1980, *The jarosite process—past, present and future*, In: Cigan, J.M., Mackey, T.S., OKeefe, T.J. (Eds.), Lead–Zinc–Tin80, TMS–AIME World Symposium on Metallurgy and Environment Control, Warrendale, PA, pp. 97–123.

BABCAN J., 1971, *Synthesis of jarosite—KFe$_3$(SO$_4$)$_2$(OH)$_6$*, Geol. Zb. 22 (2), 299–304.

BASTURKCU H. and ACARKAN N., 2016, *Leaching behaviour of a Turkish lateritic ore in the presence of additives*, Physicochem. Probl. Miner. Process. 52(1), 112−123.

BEUKES J.P., GIESEKKE E.W. and ELLIOT W. 2000, *Nickel retention by goethite and hematite*, Minerals Engineering, 13(14-15), 1573-1579.

BISWAS R.K. and BEGUM D.A., 1998, *Solvent extraction of Fe^{3+} from chloride solution by D2EHPA in kerosene*, Hydrometallurgy 50, 153–168.

BODSON F.J.J., 1972, *Recovery of zinc values from zinc plant residue*, US Patent No. 3,652, 264.

BOXAL J.M. and JAMES S.E., 1986, *Experience with the goethite process at National Zinc*, In: Dutrizac, J.E., Monhemius, A.J. (Eds.), Iron Control in Hydrometallurgy. Ellis Horwood, Chichester, UK, pp. 676–686.

BUBAN K.R., COLLINS M.J. and MASTERS I.M., 1999, *Iron control in zinc pressure leach processes*, J. Met., 51 (12), 23–25.

CARVALHO-E-SILVA M.L., RAMOS A.Y., TOLENTINO H.C.N., ENZWEILER J., NETTO S.M., ALVES M.D.C.M., 2003, *Incorporation of Ni into natural goethite: an investigation by X-ray absorption spectroscopy*, American Mineralogist, 88, 876–882.

CHANG Y., ZHAI X., LI, B. and FU Y. 2010, *Removal of iron from acidic leach liquor of lateritic nickel ore by goethite precipitate*, Hydrometallurgy, 101, 84–87.

CHEN T.T. and CABRI L.J., 1986, *Mineralogical overview of iron control in hydrometallurgical processing*, In: Dutrizac, J.E., Monhemius, A.J. (Eds.), Iron Control in Hydrometallurgy. Ellis Horwood, England, pp. 19− 55.

CORNELL R.M. and SCHWERTMANN U., 1996, *The Iron Oxides. Structure, Properties, Reactions, Occurrence and Uses*, VCH Verslagsgesellschaft, Weinheim.

CORNELL R.M. and SCHWERTMANN U., 2003, *The iron oxides: structure, properties, reactions, occurrences and uses*, Wiley-VCH GmbH and Co. KGaA, Weinheim.

CUBEDDU F., PIASENTIN M., REILLY F., MEREGALLI L. and TOLOMIO M., 1996, *The Paragoethite process at the Enirisorse–Porto Vesme plant*, In: Dutrizac, J.E., Harris, G.B. (Eds.), Proceedings of the Second International Symposium on Iron Control in Hydrometallurgy. Canadian Institue of Mining,Metallurgy and Petroleum, Ottawa, pp. 147–161.

DEMOPOULOS G.P. and GEFVERT D.L., 1984, *Iron (III) removal from base metals electrolyte solutions by solvent extraction*, Hydrometallurgy, 12, 299–315.

DUTRIZAC J.E., 1980, *The physical chemistry of iron precipitation in the zinc industry*, In: Cigan, J.M., Mackey, T.S., OKeefe, T.J. (Eds.), Lead–Zinc–Tin80, TMS–AIME World Symposium on Metallurgy and Environment Control, Warrendale, PA, pp. 532−563.

DYER L., SU B. and ASSELIN E., 2012, *Cobalt loss due to iron precipitation in ammoniacal carbonate solutions*, Hydrometallurgy, 125–126, 144–147.

FULLER C.C., DAVIS J. A. and WAYCHUNAS G.A., 1993, *Surface chemistry of ferrihydrite: Part II. Kinetics of arsenate adsorption and coprecipitation*, Geochim. Cosmochim. Acta, 57, 2271-2282.

HAIGH C. and WOOD J., 1972, *Jarosite process boosts zinc*, World Min. (September), 34–38.

HARVEY D., 2000, *Modern Analytical Chemistry*, McGraw-Hill.

HOCHELLA M.F., Jr., KASAMA T., PUTNIS A., PUTNIS C., MOORE J.N., 2005, *Environmentally important, poorly crystalline Fe/Mn hydrous oxides: Ferrihydrite and a vernadite-like mineral from a massive acid mine drainage system*, American Mineralogist, 90, 718-724.

HOH Y., WANG J. and MA T., 1983, *Solvent extraction separation study of Fe(III) and Zn(II) from aqueous solutions with D2EHPA and D2EHPA mixed with TBP in hydrocarbon diluents*, In: Proceedings of ISEC' 83.

ISMAEL M.R.C. and CARVALHO J.M.R. 2003, *Iron recovery from sulphate leach liquors in zinc hydrometallurgy*, Minerals Engineering, 16, 31–39.

JAMBOR J.L. and DUTRIZAC J.E., 1998, *Occurrence and constitution of natural and synthetic ferrihydrite, a widespread iron oxyhydroxide*, Chemical Reviews, (7), 2549–2585.

LOAN M., ST PIERRE T.G., PARKISNON G.M., NEWMAN O.M.G. and FARROW J.B., 2002, *Identifying nanoscale ferrihydrite in hydrometallurgical residues*, Journal of Metals, 54 (12), 40–43.

LOAN M., NEWMAN O.M.G., COOPER R.M.G., FARROW J.B. and PARKISNON G.M, 2006, *Defining the Paragoethite process for iron removal in zinc hydrometallurgy*, Hydrometallurgy, 81, 104–129.

LUPI C. and PILONE D., 2000, Reductive stripping in vacuum of Fe(III) from D2EHPA, Hydrometallurgy, 57 (3), 201–207.

MANCEAU P.H. and DRITIS V.A., 1993, *Local structure of ferrihydrite and feroxyhite by EXAFS spectrometer*, Clay Minerals, 28, 165-184.

MCCRISTAL T.G. and MANNING J., 1998, *Conversion of the Pasminco Hobart smelter to para-goethite*. In: Dutrizac, J.E., Gonzales, J.A., Bolton, G.L., Hancock, P. (Eds.), Zinc and Lead Processing. The Metallurgical Society of CIM, Montreal, Canada, pp. 439– 453.

MCDONALD R.G. and WHITTINGTON B.I., 2008, *Atmospheric acid leaching of nickel laterites review: Part I sulphuric acid technologies*, Hydrometallurgy, 91, 35–55.

MEALEY M., 1973, *Hydrometallurgy plays a big role in Japan's new zinc smelter*, Eng. Min. J., 174, 82–84.

MEYER E.H.O., HOWARD G., HEAGLE R. and BECK R.D., 1996, *Iron control and removal at the Zinc Corporation of South Africa*. In: Dutrizac, J.E., Harris, G.B. (Eds.), Iron control and Disposal. Canadian Institute of Mining, Metallurgy & Petroleum, Montreal, Canada, pp. 163-182.

ONAZAKI A. and KURAMOCHI S., 1986, *The Versatic acid process—a solution in the zinc industry*, In: Dutrizac, J.E., Monhemius, A.J. (Eds.), Iron Control in Hydrometallurgy. Ellis Horwood, Chichester, UK, pp. 297–311.

PAKARINEN J. and PAATERO E. 2011, *Recovery of manganese from iron containing sulfate solutions by precipitation*, Minerals Engineering, 24, 1421–1429.

PICKERING R.W. and HAIGH C.J., 1970, *Treatment of zinc plant residue*, US Patent No. 3, 493, 365.

PRESTON J.S., 1985, *Solvent extraction of metals by carboxylic acids*, Hydrometallurgy, 14, 171–188.

RITCEY G.M., 2006, *Solvent extraction, principles and application to process metallurgy*, Vol. 1, 2nd ed. G.M. Ritcey & Associates incorporation, Ottawa.

ROPENAC A.V., 1986, *Hematite—the solution to a disposal problem—an example from the zinc industry*, In: Dutrizac, J.E., Monhemius, A.J. (Eds.), Iron Control in Hydrometallurgy. Ellis Horwood, Chichester, UK, pp. 730–741.

SATO T. and NAKAMURA T., 1971, *Extraction of iron (III) from sulphuric and hydrochloric acid solutions by di-2(ethylhexyl)phosphoric acid*, In: Proceedings of ISEC' 71, vol. 1. Society of Chemical Industry, London, pp. 238–248.

SATO T., NAKAMURA T. and IKENO M., 1985, *The extraction of iron (III) from aqueous acid solutions by di(2-ethylhexyl)phosphoric acid*, Hydrometallurgy, 15, 209–217.

SAJI J., RAO T.P., IYER C.S.P. and REDDY M.L.P., 1998, *Extraction of iron(III) from acidic chloride solutions by Cyanex 923*, Hydrometallurgy, 49, 289–296.

SCOTT J.D., DONYINA D.K.A. and MOULAND J.E., 1986, *Iron-the good with the bad—Kidd Creek zinc plant experience*, In: Dutrizac, J.E., Monhemius, A.J. (Eds.), Iron Control in Hydrometallurgy. Ellis Horwood, Chichester, UK, pp. 666–675.

SCHWERTMANN U. and R. M. CORNELL. 1991, *Iron Oxides in the Laboratory*, Weinheim: VCH, Weinheim City in Germany, 89-94.

SINGH B., SHERMAN D.M., GILKES R.J., WELLS M.A. and MOSSELMANS J.F.W., 2002, *Incorporation of Cr, Mn and Ni into goethite (a-FeOOH): mechanism from extended X-ray absorption fine structure spectroscopy*, Clay Minerals 37, 639–649.

STEINTVEIT G., 1971, *Treatment of zinc leach plant residue by the jarosite process*, In: Advances in Extractive Metallurgy and Refining. IMM, London, pp. 521–528.

TORFS K.J., VLIEGEN J., 1996, *The Union Miniere Goethite process: plant practice and future prospects*, In: Dutrizac, J.E., Harris, G.B. (Eds.), Iron Control and Disposal. The Canadian Institute of Mining, Metallurgy and Petroleum, Montreal, Canada, pp. 135–146.

VAZARLIS H. and NEOU-SYNGGOYNA P., 1984, *A study of the leaching of Cu and Zn from Greek copper concentrate. Liquid–liquid extraction for the separation of Cu, Zn and Fe from leach solutions*, Hydrometallurgy 12, 365–373.

WANG K., LI J., MCDONALD R.G., BROWNER R.E., 2011, *The effect of iron precipitation upon nickel losses from synthetic atmospheric nickel laterite leach solutions: statistical analysis and modelling*, Hydrometallurgy, 109, 140–152.

WANG K., LI J., MCDONALD R.G., BROWNER R.E., 2013, *Characterisation of iron-rich precipitates from synthetic atmospheric nickel laterite leach solutions*, Minerals Engineering 40, 1–11.

WAYCHUNAS G.A., REA B.A., FULLER C.C. and DAVIS J.A., 1993, *Surface chemistry of ferrihydrite: Part I. EXAFS studies of the geometry of coprecipitated and adsorbed arsenate*, Geochim. Cosmochim. Acta, 57,2251-2269.

WELCH A.H., WESTJOHN D.B., HELSEL D.R. and WANTY R.B., 2000, *Arsenic in ground water of the United States-- occurrence and geochemistry*, Ground Water, 38(4), 589-604.

ZHOU T., ZHONG X. and ZHENG L., 1989, *Recovering In, Ge, Ga from zinc residues*, J. Met., 36–40.